

Kohn-Luttinger mechanism driven exotic topological superconductivity on the Penrose lattice

Ye Cao,¹ Yongyou Zhang,¹ Yu-Bo Liu,¹ Cheng-Cheng Liu,¹ Wei-Qiang Chen,² and Fan Yang^{1,*}

¹*School of Physics, Beijing Institute of Technology, Beijing 100081, China*

²*Department of Physics, Southern University of Science and Technology, Shenzhen, China*

(Dated: January 26, 2025)

The Kohn-Luttinger mechanism for unconventional superconductivity (SC) driven by weak repulsive electron-electron interactions on a periodic lattice is generalized to the quasi crystal via a real-space perturbative approach. The repulsive Hubbard model on the Penrose lattice is studied as an example, on which a classification of the pairing symmetries is performed and a pairing phase diagram is obtained. Two remarkable properties of these pairing states are revealed, due to the combination of the presence of the point-group symmetry and the lack of translation symmetry on this lattice. Firstly, the spin and spacial angular momenta of a Cooper pair is de-correlated: for each pairing symmetry, both spin-singlet and spin-triplet pairings are possible even in the weak-pairing limit. Secondly, the pairing states belonging to the 2D irreducible representations of the D_5 point group can be time-reversal-symmetry-breaking topological SCs carrying spontaneous bulk super current and spontaneous vortices. These two remarkable properties are general for the SCs on all quasi-crystals, distinguished from those on periodic lattices and strong-disorder-limit solids.

Introduction: The quasi-crystal (QC) have attracted a lot of research interests[1] since synthesized[2]. The QC represents a certain type of solid structures which are lack of translation symmetry but can possess rotation symmetries such as the five-folded or eight-folded ones forbidden by crystalline point group[2]. The electronic structure on a QC is exotic and fundamentally different from that on a crystal. Particularly, due to the lack of translation symmetry on a QC, the lattice momentum is no longer a good quantum number and no Fermi surface (FS) can be defined. Various exotic quantum states with intriguing properties have been revealed on the QC recently[3–25]. Particularly, the definite experimental evidences for superconductivity (SC) in the recently synthesized Al-Zn-Mg QC[26], together with those in previous ternary QCs[27, 28] and crystalline approximants[29], have attracted a lot of research interests[30–33]. It’s interesting to ask a question here: are there any common features of superconducting states on the QC which are fundamentally different from those on a crystal?

In Ref [33], the pairing state for an attractive Hubbard model is studied on a Penrose lattice, i.e. a QC with five-folded rotation symmetry. It’s found that a weak attraction can lead to Cooper instability [34] between a time-reversal (TR) partners, obeying the Anderson’s theorem [35]. Further more, despite the lack of lattice momentum on the QC, the Cooper pairing can lead to a finite superfluid density. These results suggest that the SC on the QC with attractive interactions is similar with that in a strong-disorder-limit solid, consistent with the BCS theory [30]. However, the situation is distinct for the cases with repulsive interactions, as will be shown below. The pairing in the presence of weak repulsive interactions is induced by the Kohn-Luttinger (KL) mechanism

[1, 2]. This theory states that the interaction renormalization brought about by exchanging particle-hole excitations is anisotropic on the FS, which can generate some attractive-interaction channels between the TR partners, which finally leads to Cooper pairing on the FS. Here, we generalize this mechanism to the QC, and obtain unconventional SCs with a series of remarkable properties intrinsic to the QCs which are absent in periodic lattices or strong-disorder-limit solids.

In this paper, we study the KL SC in a weak-U repulsive Hubbard model on a Penrose lattice. Via a real-space perturbative treatment up to the second order, we acquire an effective interaction vertex, through which we derive a linearized gap equation near the superconducting critical temperature T_c , solving which we obtain the T_c and the pairing gap functions. We classify the pairing symmetries and obtain the pairing phase-diagram after large scale numerical calculations. Two remarkable results are obtained. Firstly, the spacial- and spin- angular momenta of the Cooper pair are de-correlated, which means that we can obtain both spin-singlet and spin-triplet pairings for the same pairing symmetry, distinguished from the case on a periodic lattice in the weak-pairing limit. Secondly, any 2D irreducible representation (IR) of the D_5 point group can bring about TR symmetry (TRS)-breaking topological SCs (TSCs) hosting spontaneous bulk super current and spontaneous vortices. These two properties are caused by the combination of the point-group symmetry and the lack of translation symmetry, and are thus general for the SCs on any QC, distinguished from those on periodic lattices or in strong-disorder-limit solids.

Model and Approach: Let’s consider the following standard repulsive Hubbard model on the Penrose lattice [38] shown in Fig. 1(a),

$$\hat{\mathcal{H}} = - \sum_{i,j,\sigma} t_{ij} c_{i\sigma}^\dagger c_{j\sigma} + U \sum_i n_{i\uparrow} n_{i\downarrow} - \mu \sum_{i,\sigma} n_{i\sigma}, \quad (1)$$

* yangfan_blg@bit.edu.cn

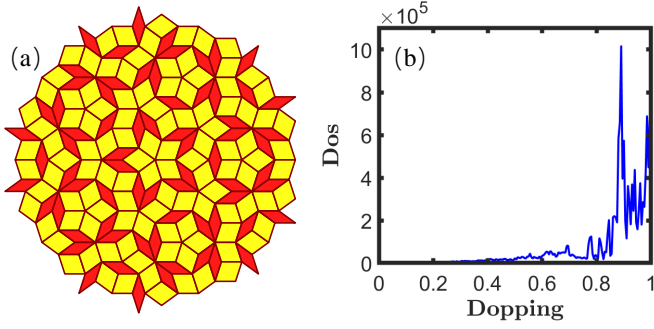


Figure 1. (Color online) Lattice pattern with 191 points (a) and the density of state (DOS) of tight-binding Hamiltonian on a lattice with 13926 sites (b). The hopping integral adopted is $t_{ij} = e^{-|\mathbf{i}-\mathbf{j}|/\min|\mathbf{i}-\mathbf{j}|}$ for $\mathbf{i} \neq \mathbf{j}$.

where $c_{i\sigma}$ annihilates an electron at site \mathbf{i} with spin σ , $n_{i\sigma}$ is the electron-number operator, and μ denotes the chemical potential. The hopping integral t_{ij} adopted is $t_{ij} \propto e^{-|\mathbf{i}-\mathbf{j}|/\min|\mathbf{i}-\mathbf{j}|}$, where $|\mathbf{i}-\mathbf{j}|$ denotes the distance between different sites \mathbf{i} and \mathbf{j} . The tight-binding (TB) model as the kinetic part of Eq.(1) can be diagonalized as $\hat{H}_{\text{TB}} = \sum_m \tilde{\epsilon}_m c_{m\sigma}^\dagger c_{m\sigma}$, with $c_{m\sigma} = \sum_{\mathbf{i}} \xi_{im} c_{i\sigma}$. Here m labels a single-particle eigen state with energy $\tilde{\epsilon}_m = \epsilon_m - \mu$ relative to the chemical potential, and ξ_{im} represents for the wave function for the state m . The single-particle density of states (DOS) shown in Fig.1(b) peaks at around the filling fraction of 0.9, which will be focused on below. In unit of the largest hopping integral, the total band width W is about 2.44. We consider weak $U > 0$ and adopt perturbative approach in our work.

For this repulsive Hubbard model, SC is forbidden in the mean-field (MF) level. However, it can be driven by the KL mechanism, wherein unconventional SC is mediated by exchanging spin or charge fluctuations in the particle-hole channel. Due to the lack of translation symmetry, we engage a real-space perturbative treatment, whose details are provided in the Supplementary Material (SM)[39]. The real-space propagator of the particle-hole fluctuations is described by the susceptibility function, which in the bare level reads[39]

$$\begin{aligned} \chi_{ij}^{(0)}(i\Omega_n) &= \int_0^\beta e^{i\Omega_n\tau} d\tau \langle T_\tau c_{i\uparrow}^\dagger(\tau) c_{i\uparrow}(\tau) c_{j\uparrow}^\dagger c_{j\uparrow} \rangle_0 \\ &= \sum_{ml} \xi_{im} \xi_{jm} \xi_{il} \xi_{jl} \frac{n_F(\tilde{\epsilon}_m) - n_F(\tilde{\epsilon}_l)}{i\Omega_n + \tilde{\epsilon}_l - \tilde{\epsilon}_m}. \end{aligned} \quad (2)$$

In our calculations, only about a 1000×1000 number of (m, l) near the Fermi level are summed in Eq. (2). In our perturbative treatment (see the SM), the four second-order processes of exchanging particle-hole fluctuations induce effective interactions, from which we obtain[39]

$$\begin{aligned} \hat{H}_{eff} &= - \sum_{\mathbf{i}, \mathbf{j}, \sigma} t_{ij} c_{i\sigma}^\dagger c_{j\sigma} + U \sum_{\mathbf{i}} n_{i\uparrow} n_{i\downarrow} - \mu \sum_{\mathbf{i}, \sigma} n_{i\sigma} \\ &\quad - (U^2/2) \sum_{\mathbf{i}, \mathbf{j}, \sigma, \sigma'} \chi_{ij} c_{i\sigma}^\dagger c_{i\sigma'} c_{j\sigma'}^\dagger c_{j\sigma}. \end{aligned} \quad (3)$$

with $\chi_{ij} \equiv \chi_{ij}^{(0)}(i\Omega_n = 0)$. The induced term with coefficient $-(U^2/2)$ in Eq. (3) can drive SC in the MF level.

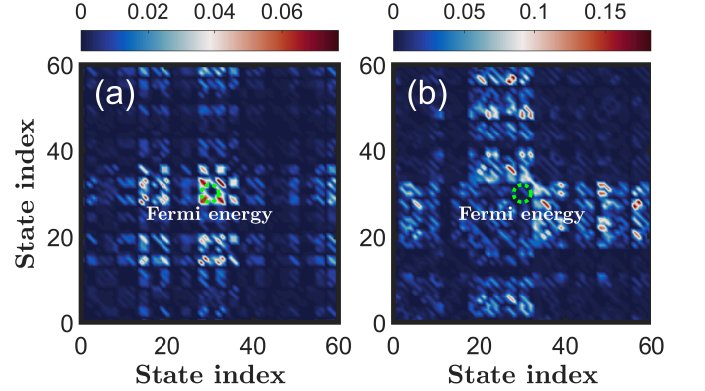


Figure 2. (Color online) Contour plots of relative $|\tilde{\Delta}_{mn}|$ for a singlet s/h state (a, doping=0.81, $U/W_D = 0.32$) and a triplet $d + id/f + if$ state (b, doping=0.98, $U/W_D = 0.32$).

A BCS-MF study is performed on Eq. (3). See the SM for more details. Noting that the Cooper pairing can only take place near the Fermi level, we transform the real-space pairing order parameter Δ_{ij} into the m -space as $\tilde{\Delta}_{mn}$ and maintain those m/n -states within a narrow energy shell near the Fermi level. A self-consistent MF equation for $\tilde{\Delta}_{mn}$ is obtained at any temperature, leading to the following linearized equation at T_c [39],

$$\sum_{m'n'} F_{mn, m'n'} \tilde{\Delta}_{m'n'} = \tilde{\Delta}_{mn}, \quad (4)$$

with $\tilde{\Delta}_{mn} = \tilde{\Delta}_{mn} f_{mn}$, where

$$f_{mn} = \sqrt{(n_F(-\tilde{\epsilon}_n) - n_F(\tilde{\epsilon}_m)) / (\tilde{\epsilon}_m + \tilde{\epsilon}_n)}. \quad (5)$$

The formula $F_{mn, m'n'}$ for the singlet pairing is given as

$$\begin{aligned} F_{mn, m'n'}^{(s)} &= -f_{mn} f_{m'n'} \left[U \sum_{\mathbf{i}} \xi_{im} \xi_{in} \xi_{im'} \xi_{in'} \right. \\ &\quad \left. + \frac{U^2}{4} \sum_{\mathbf{i}, \mathbf{j}} \chi_{ij} (\xi_{im} \xi_{jn} + \xi_{in} \xi_{jm}) (m, n \Rightarrow m', n') \right], \end{aligned} \quad (6)$$

and for the triplet case it is

$$\begin{aligned} F_{mn, m'n'}^{(t)} &= f_{mn} f_{m'n'} \left[\frac{U^2}{4} \sum_{\mathbf{i}, \mathbf{j}} \chi_{ij} (\xi_{im} \xi_{jn} \right. \\ &\quad \left. - \xi_{in} \xi_{jm}) (m, n \Rightarrow m', n') \right]. \end{aligned} \quad (7)$$

The linearized gap equation (4) takes the form of an eigenvalue problem of the matrix $F_{mn, m'n'}$ (here we take the combined mn or $m'n'$ as one index), wherein its largest eigenvalue attains 1 at T_c , with the corresponding eigenvector $\tilde{\Delta}_{mn}$ determining the pairing symmetry. Due to the lack of translation symmetry here, the real-space

Table I. IRs of the D_5 point group and classification of pairing symmetries. \hat{R}_θ denotes the rotation about the center of the Penrose lattice by the angle $\theta = 2n\pi/5$ and $\hat{\sigma}$ represents the reflection about any of the five symmetric axes. $D^{(C_{2\pi/5})}$ and $D^{(\sigma_x)}$ are the representation matrices for the two generators of D_5 , i.e. $C_{2\pi/5}$ and σ_x , up to any unitary transformation. For each pairing symmetry listed, both spin-singlet and spin-triplet pairings are possible.

IRs	$D^{(C_{2\pi/5})}$	$D^{(\sigma_x)}$	pairing symmetries	ground-state gap functions
1D	A_1	I	s or $h_{x^5-10x^3y^2+5xy^4}$	$\Delta_{\hat{R}_\theta i, \hat{R}_\theta j} = \Delta_{i,j}$, $\Delta_{\hat{\sigma} i, \hat{\sigma} j} = \Delta_{i,j}$
	A_2	I	$h'_{y^5-10x^2y^3+5x^4y}$ or $h \cdot h'$	$\Delta_{\hat{R}_\theta i, \hat{R}_\theta j} = \Delta_{i,j}$, $\Delta_{\hat{\sigma} i, \hat{\sigma} j} = -\Delta_{i,j}$
2D	E_1	$\cos \frac{2\pi}{5} I \pm i \sin \frac{2\pi}{5} \sigma_y$	(p_x, p_y) or $(g_{x^4-6x^2y^2+y^4}, g_{4x^3y-4xy^3})$	$\Delta_{\hat{R}_\theta i, \hat{R}_\theta j} = e^{\pm i\theta} \Delta_{i,j}$, $\Delta_{\hat{\sigma} i, \hat{\sigma} j} \neq \pm \Delta_{i,j}$
	E_2	$\cos \frac{4\pi}{5} I \pm i \sin \frac{4\pi}{5} \sigma_y$	$(d_{x^2-y^2}, d_{2xy})$ or $(f_{x^3-3xy^2}, f_{3x^2y-y^3})$	$\Delta_{\hat{R}_\theta i, \hat{R}_\theta j} = e^{\pm 2i\theta} \Delta_{i,j}$, $\Delta_{\hat{\sigma} i, \hat{\sigma} j} \neq \pm \Delta_{i,j}$

gap function $\Delta_{i,j}$ is no longer just a function of $\mathbf{i} - \mathbf{j}$, but a binary function of both \mathbf{i} and \mathbf{j} . The situation is similar in the m -space. The m, n -dependence of $|\tilde{\Delta}_{mn}|$ is shown in Fig. 2 for two typical solutions solved from Eq. (4), where for each m there is no unique n which makes $|\tilde{\Delta}_{mn}|$ dominate that of any other n , distinct from the result for $U < 0$ wherein $|\tilde{\Delta}_{mm}| \gg |\tilde{\Delta}_{mn}(n \neq m)|$ [33]. Such a behavior breaks the Anderson's theorem applied for the strong-disorder-limit superconductors, which states that an electron state can only pair with its TR-partner.

Pairing symmetries and phase-diagram: The classification of pairing symmetries here is based on the symmetry of the linearized gap equation (4)[39]. It's proved that the ‘‘pairing potential’’ $F_{mn,m'n'}$ is invariant under the D_5 point group. Consequently, the set of solutions $\{\tilde{\Delta}_{mn}^{(\alpha)}\}$ ($\alpha = 1$ or 2) of Eq. (4) corresponding to the same T_c furnish an IR of D_5 . This statement also holds for the real-space gap function $\Delta_{i,j}^{(\alpha)}$ [39]:

$$\Delta_{gi,gj}^{(\alpha)} = \sum_{\alpha'} D_{\alpha\alpha'}^{(g)} \Delta_{i,j}^{(\alpha')}, \quad (8)$$

with any $g \in D_5$. Then, from the IR which the set of matrices $\{D^{(g)}\}$ belong to, one can judge the pairing symmetry of the state with gap function $\Delta_{i,j}^{(\alpha)}$.

The four IRs of the D_5 point group are listed in Table I, including two 1D IRs, i.e. A_1 and A_2 , and two 2D IRs, i.e. E_1 and E_2 . For each IR, we list the representation matrices for the two generators of D_5 , i.e. the $C_{2\pi/5}$ and σ_x , up to an arbitrary unitary transformation. Each IR listed in Table I corresponds to one pairing-symmetry class. The identity representation A_1 is naturally viewed as the s -wave with angular momentum $l = 0$. However, it can also be equally viewed as the $h_{x^5-10x^3y^2+5xy^4}$ -wave with $l = 5$ which is σ -reflection even, because on the Penrose lattice with 5-folded rotation symmetry the s - and h -waves are both invariant under each $2\pi/5$ -rotation. The A_2 representation is the $h'_{y^5-10x^2y^3+5x^4y}$ -wave with $l = 5$ which is σ -reflection odd. The E_1 (E_2) representation provides the doubly-degenerate p -wave (d -wave) with $l = 1$ ($l = 2$), or equally the doubly-degenerate g -wave (f -wave) with $l = 4$ ($l = 3$).

Note that for each of the pairing symmetry listed in Table I, both spin-singlet and spin-triplet pairings

are possible. This remarkable result suggests the decorelation between the spacial- and the spin- angular momenta of a Cooper pair on the QC lattices, distinguished from the situations on periodic lattices. Generally, in a spin-singlet (triplet) pairing state where the spin part of the Cooper-pair wave function is exchange- odd (even), the Fermi statistics requires the spacial part to be exchange- even (odd), i.e. $\Delta_{i,j} = \Delta_{j,i}$ ($\Delta_{i,j} = -\Delta_{j,i}$). On periodic lattices, the translation symmetry requires $\Delta_{j,i} = \Delta_{-i,-j} = \Delta_{j-i}$. Consequently, in a singlet (triplet) pairing state, we have $\Delta_{i,j} = \Delta_{-i,-j}$ ($\Delta_{i,j} = -\Delta_{-i,-j}$), implying an even (odd) spacial angular momentum. Such a definite correlation between the spin- and spacial- angular momenta of the Cooper pair holds even for a complex periodic lattice with multi orbitals in the weak-pairing limit, wherein the pairing always takes place within intra-band. However, in the QC lattice studied here without translation symmetry, we have $\Delta_{j,i} \neq \Delta_{-i,-j}$ and therefore the relation between $\Delta_{i,j}$ and $\Delta_{-i,-j}$ is not correlated with the spin degree of freedom. What's more, the ‘‘intra-band’’ pairing doesn't make sense here.

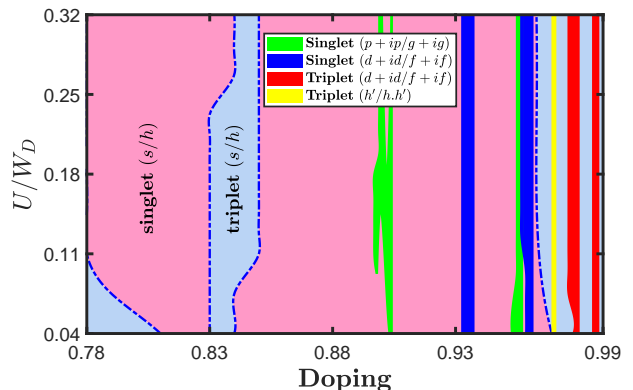


Figure 3. (Color online) Ground-state pairing phase diagram in the doping-interaction plane. The interaction strength of U is limited within a weak-coupling range of $(0, W_D/3)$.

The pairing phase diagram is shown in Fig. 3 obtained through solving Eq. (4) for the singlet and triplet channels separately. In our calculations, we adopt a lattice with 13926 sites with open-boundary condition. We focus on the doping range of $(0.78, 0.99)$ wherein the

DOS is the largest and the T_c is relatively high. The Hubbard- U adopted here is within a weak-coupling range of $(0, W_D/3)$. For the sake of reducing the computation complexity, we limit the states marked by $m^{(l)}/n^{(l)}$ in Eq. (4) to Eq. (7) within a narrow energy window near the Fermi level containing about 100 states. From Fig. 3, the obtained pairing symmetries slightly depend on U/W_D but strongly depend on the doping level. Six out of the eight possible pairing states listed in Table I are obtained, including the singlet and triplet s/h - and d/f -waves, the singlet p/g -wave and the triplet $h'/h \cdot h'$ -wave pairing symmetries.

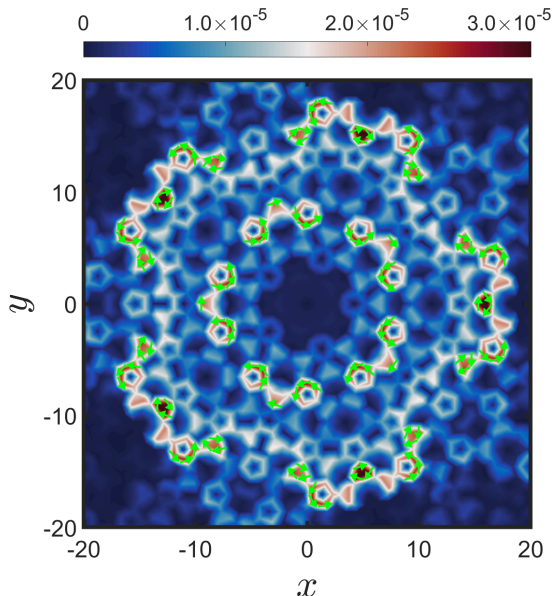


Figure 4. (Color online) Contour plot of the amplitude of the spontaneous bulk super current in the same pairing state as that in Fig. 2 (b). The green arrows indicate the direction of the current at a specific site. To enhance the visibility, only typical sites are marked with the direction of the current.

Exotic TSCs: The spin-singlet and spin-triplet p/g - and d/f -wave pairings states listed in Table I or Fig. 3 belong to 2D IRs of the point group, suggesting the existence of doubly degenerate gap functions $\Delta_{mn}^{(1,2)}$, which would be mixed below T_c to lower the free energy. At $T = 0$, the minimization of the expectation value of the effective Hamiltonian (3) in the BdG MF ground state with gap form factor $\Delta_{mn}^{(1)} + \alpha \Delta_{mn}^{(2)}$ yields $\alpha = \pm i$ for all these cases. Therefore such degenerate doublets would be mixed as $p+ip/g+ig$ and $d+id/f+if$ in the ground state. The real-space gap functions $\Delta_{\mathbf{i},\mathbf{j}} = \Delta_{\mathbf{i},\mathbf{j}}^{(1)} \pm i\Delta_{\mathbf{i},\mathbf{j}}^{(2)}$ of these mixed states show nontrivial winding-number structures: with each θ -angle rotation ($\theta = 2n\pi/5$) about the lattice center performed on combined (\mathbf{i},\mathbf{j}) , the complex phase of $\Delta_{\mathbf{i},\mathbf{j}}$ would be shifted by $\pm l\theta$ (l is the spacial angular momentum of the pairing), as listed in Table I. Such nontrivial winding numbers of these pairing states suggest that they are topologically nontrivial.

To better characterize the topology of these pairing

states on the QC without translation symmetry[3, 4], we use the K -theory class characterized by the Chern number. On the finite lattice, based on the spectral-localizer method, the Chern number is obtained as the following pseudo-spectrum invariant index C_{ps} [39],

$$C_{ps} = \frac{1}{2} \text{Sig} \begin{pmatrix} X & Y + iH \\ Y - iH & -X \end{pmatrix}. \quad (9)$$

Here X and Y are the position operators, H is the BdG-Hamiltonian matrix and Sig represents the difference between the numbers of positive and negative eigenvalues of the matrix acted on [39]. Using this formula, we obtain the following two universal results (proved in the SM[39]). Firstly, the C_{ps} of all 1D-IR pairing states are zero. Secondly, for triplet pairing states belonging to the 2D-IRs, the C_{ps} for the TRS-breaking chiral-pairing states $\sum_{\mathbf{i},\mathbf{j}} \Delta_{\mathbf{i},\mathbf{j}}(c_{\mathbf{i}\uparrow}c_{\mathbf{j}\downarrow} + c_{\mathbf{i}\downarrow}c_{\mathbf{j}\uparrow}) + h.c.$ (or $\sum_{\mathbf{i},\mathbf{j}} \Delta_{\mathbf{i},\mathbf{j}}(c_{\mathbf{i}\uparrow}c_{\mathbf{j}\uparrow} \pm c_{\mathbf{i}\downarrow}c_{\mathbf{j}\downarrow}) + h.c.$) are twice of those for the spinless system with $\sum_{\mathbf{i},\mathbf{j}} \Delta_{\mathbf{i},\mathbf{j}}c_{\mathbf{i}}c_{\mathbf{j}} + h.c.$, and those for the TRI helical-pairing states $\sum_{\mathbf{i},\mathbf{j}} (\Delta_{\mathbf{i},\mathbf{j}}c_{\mathbf{i}\uparrow}c_{\mathbf{j}\uparrow} \pm \Delta_{\mathbf{i},\mathbf{j}}^*c_{\mathbf{i}\downarrow}c_{\mathbf{j}\downarrow}) + h.c.$ are zero. These triplet pairing states are degenerate here without considering the spin-orbit coupling. Our numerical calculations on the 2D-IR singlet and chiral-triplet pairing states appearing in the phase diagram yield that their Chern numbers are generally integer multiples of twice of their spacial angular momenta, suggesting the presence of TSCs without translation symmetry.

A general and remarkable property of the TSCs on a QC is the presence of spontaneous bulk super current caused by the lack of translation symmetry, distinguished from a periodic lattice. To illustrate this, we have calculated the expectation values of the site-dependent current operator $\hat{\mathbf{J}}_{\mathbf{i}} = -\delta\hat{\mathcal{H}}/\delta\mathbf{A}_{\mathbf{i}}|_{\mathbf{A}=0} = \frac{i}{2} \sum_{\mathbf{j}\sigma} t_{\mathbf{i}\mathbf{j}}(\mathbf{r}_{\mathbf{j}} - \mathbf{r}_{\mathbf{i}})c_{\mathbf{i}\sigma}^\dagger c_{\mathbf{j}\sigma} + h.c.$ (see [39]). Note that $\hat{\mathbf{J}}_{\mathbf{i}}$ is TR odd, whose expectation value $\langle \hat{\mathbf{J}}_{\mathbf{i}} \rangle$ should be zero in TRI states. However, in the TRS-breaking chiral pairing states belonging to the 2D-IR, our numerical results shown in Fig. 4 illustrates a five-fold-symmetric pattern with $\langle \hat{\mathbf{J}}_{\mathbf{i}} \rangle \neq 0$ for any typical site. It's intriguing that the super current forms spontaneous vortices here and there, leading to bulk orbital magnetization that can be detected by experiments. Note that $\sum_{\mathbf{i}} \langle \hat{\mathbf{J}}_{\mathbf{i}} \rangle = 0$, otherwise the macro superfluid density (see below) would be infinity. Such spontaneous bulk super current and vortices are absent in translation-symmetric systems in the continuum limit, because the spontaneous super current there can only emerge at the edge or around the dislocations where the translation symmetry is broken [42–47], leading to difficulty in its experimental detection [48–50]. Here the lack of translation symmetry on the QC leads to spontaneous super current everywhere in the bulk.

Discussion and Conclusion: One might wonder whether the lack of translation symmetry on the Penrose lattice would destroy the phase coherence of the

pairing state. This puzzle can be settled by investigating the superfluid density ρ_s defined as $\rho_s^{\alpha\beta} \equiv \lim_{\mathbf{A} \rightarrow 0} \frac{-\langle \mathbf{A} | \hat{J}_\alpha[\mathbf{A}] | \mathbf{A} \rangle}{A_\beta}$, with $\alpha/\beta = x, y$ [39]. Here a weak uniform vector potential \mathbf{A} along the β -direction is coupled with the system, $\hat{\mathbf{J}}[\mathbf{A}] = -\delta\hat{\mathcal{H}}[\mathbf{A}]/\delta\mathbf{A}$ and $|\mathbf{A}\rangle$ represents the ground state of $\hat{\mathcal{H}}[\mathbf{A}]$. It's proved here[39] that $\rho_s^{\alpha\beta} = \rho_0\delta_{\alpha\beta}$ and our numerical result yields $\rho_0 > 0$, suggesting a true superconducting state with nonzero superfluid density and hence measurable Meissner effect.

The real-space perturbative approach engaged here and the insight acquired from this work would also apply to other QCs. Particularly, the recently synthesized 30°-twisted bilayer graphene[51, 52] provides a relevant platform for the QC Hubbard model studied here. Similar exotic TSCs would be detected there with proper doping. More interestingly, the D_{12} point group of that QC system leads to more IRs than those of the Penrose lattice. Consequently, exotic TSCs with winding numbers of 3, 4 and 5 are possible, higher than the 1 ($p+ip$) or 2 ($d+id$) obtained here or in periodic systems.

In conclusion, we have performed a real-space pertur-

bative calculation for the Hubbard model on the Penrose lattice. Our results reveal various classes of unconventional SCs induced via the Kohn-Luttinger mechanism. We have classified the pairing symmetries according to the IRs of the D_5 point group of this lattice, with most of them exhibited in the pairing phase diagram. Remarkably, each pairing symmetry can be both spin-singlet and spin-triplet. All the 2D-IR pairing states can be TRS-breaking chiral TSCs hosting spontaneous bulk super current and spontaneous vortices. These exotic properties of the SCs on the Penrose lattice are caused by the combination of the point-group symmetry and the lack of translation symmetry, and are thus general for all QC lattices, different from those on periodic lattices and in strong-disorder-limit superconductors.

ACKNOWLEDGEMENTS

We acknowledge stimulating discussions with Wen Huang. This work is supported by the NSFC (Grant Nos. 11704029, 11674025, 11922401).

-
- [1] See, A. I. Goldman and R. F. Kelton, Rev. Mod. Phys. 65, 213 (1993) and the references there.
 - [2] D. Shechtman, I. Blech, D. Gratias, and J. W. Cahn, Phys. Rev. Lett. 53, 1951 (1984).
 - [3] H. Tsunetsugu, T. Fujiwara, K. Ueda, T. Tokihiro, Phys. Rev. B 43, 8879 (1991).
 - [4] H. Tsunetsugu, K. Ueda, Phys. Rev. B 43, 8892 (1991).
 - [5] Susumu Yamamoto and Takeo Fujiwara, Phys. Rev. B 51, 8841 (1995).
 - [6] S. Wessel, A. Jagannathan, and S. Haas, Phys. Rev. Lett. 90, 177205 (2003).
 - [7] S. Thiem and J. T. Chalker, Phys. Rev. B 92, 224409 (2015).
 - [8] A. Koga and H. Tsunetsugu, Phys. Rev. B 96, 214402 (2017).
 - [9] J. Otsuki and H. Kusunose, J. Phys. Soc. Jap. 85, 073712 (2016).
 - [10] S. Watanabe and K. Miyake, J. Phys. Soc. Jap. 85, 063703 (2016).
 - [11] V. R. Shaginyan, A. Z. Msezane, K. G. Popov, G. S. Japaridze, and V. A. Khodel, Phys. Rev. B 87, 245122 (2013).
 - [12] N. Takemori and A. Koga, J. Phys. Soc. Jap. 84, 023701 (2015).
 - [13] S. Takemura, N. Takemori, and A. Koga, Phys. Rev. B 91, 165114 (2015).
 - [14] E. C. Andrade, A. Jagannathan, E. Miranda, M. Vojta, and V. Dobrosavljevic, Phys. Rev. Lett. 115, 036403 (2015).
 - [15] Y. E. Kraus, Y. Lahini, Z. Ringel, M. Verbin, and O. Zeitler, Phys. Rev. Lett. 109, 106402 (2012).
 - [16] H. Huang and F. Liu, Phys. Rev. Lett. 121, 126401 (2018).
 - [17] H. Huang and F. Liu, Phys. Rev. B 100, 085119 (2019).
 - [18] S. Longhi, Phys. Rev. Lett. 122, 237601 (2019).
 - [19] S. Autti, V. B. Eltsov, and G. E. Volovik, Phys. Rev. Lett. 120, 215301 (2018).
 - [20] K. Giergiel, A. Kuros, and K. Sacha, Phys. Rev. B 99, 220303 (2019).
 - [21] L.-J. Lang, X. Cai, and S. Chen, Phys. Rev. Lett. 108, 220401 (2012).
 - [22] L. Sanchez-Palencia and L. Santos, Phys. Rev. A 72, 053607 (2005).
 - [23] K. Singh, K. Saha, S. A. Parameswaran, and D. M. Weld, Phys. Rev. A 92, 063426 (2015).
 - [24] M. A. Bandres, M. C. Rechtsman, and M. Segev, Phys. Rev. X 6, 011016 (2016) (2016).
 - [25] J. Hou, H. Hu, K. Sun, and C. Zhang, Phys. Rev. Lett. 120, 060407 (2018).
 - [26] K. Kamiya, T. Takeuchi, N. Kabeya, N. Wada, T. Ishimasa, A. Ochiai, K. Deguchi, K. Imura, and N. K. Sato, Nat. Commun. 9, (2018).
 - [27] K. M. Wong, E. Lopdrup, J. L. Wagner, Y. Shen, and S. J. Poon, Phys. Rev. B 35, 2494 (1987).
 - [28] J. L. Wagner, B. D. Biggs, K. M. Wong, and S. J. Poon, Phys. Rev. B 38, 7436 (1988).
 - [29] K. Deguchi, M. Nakayama, S. Matsukawa, K. Imura, K. Tanaka, T. Ishimasa, and N. K. Sato, J. Phys. Soc. Jap. 84, 023705 (2015).
 - [30] R. N. Araújo and E. C. Andrade, Phys. Rev. B 100, 014510 (2019).
 - [31] S. Sakai and R. Arita, Phys. Rev. Res. 1, 1 (2019).
 - [32] Y. Nagai, arXiv:2001.02362.
 - [33] Y.-Y. Zhang, Y.-B. Liu, W.-Q. Chen and F. Yang, arXiv:1808.08001.
 - [34] L. N. Cooper, Phys. Rev. 104, 1189 (1956).
 - [35] P. W. Anderson, J. Phys. Chem. Solids. 11, 26 (1959).
 - [36] W. Kohn and J. M. Luttinger, Phys. Rev. Lett. 15, 524 (1965).
 - [37] M. A. Baranov, A. V. Chubukov, and M. Yu. Kagan, Int. J. Mod. Phys. B 06, 2471 (1992).

- [38] Roger Penrose, The Role of Aesthetics in Pure, and Applied Mathematical Research, Bull. Inst. Math. Appl. **10**, 266 (1974).
- [39] See the Supplementary Material at for our real-space perturbative theory on the repulsive Hubbard model, the basis for the classification of pairing symmetries on the QC, the definition and properties of the topological invariant and the current operator.
- [40] T. A. Loring, Ann. Phys. (N. Y). **356**, 383 (2015).
- [41] I. C. Fulga, D. I. Pikulin, and T. A. Loring, Phys. Rev. Lett. **116**, 257002 (2016).
- [42] B. Horowitz and A. Golub, Phys. Rev. B **68**, 214503 (2003).
- [43] M. Stone and R. Roy, Phys. Rev. B **69**, 184511 (2004).
- [44] B. Braunecker, P. A. Lee, and Z. Wang, Phys. Rev. Lett. **95**, 017004 (2005).
- [45] J. A. Sauls, Phys. Rev. B **84**, 214509 (2011).
- [46] C. Kallin, Rep. Prog. Phys. **75**, 042501 (2012).
- [47] W. Huang, E. Taylor, and C. Kallin, Phys. Rev. B **90**, 224519 (2014).
- [48] K. D. Nelson, Z. Q. Mao, Y. Maeno, and Y. Liu, Science **306**, 1151 (2004).
- [49] J. R. Kirtley, C. Kallin, C. W. Hicks, E.-A. Kim, Y. Liu, K. A. Moler, Y. Maeno, and K. D. Nelson, Phys. Rev. B **76**, 014526 (2007).
- [50] P. J. Curran, S. J. Bending, W. M. Desoky, A. S. Gibbs, S. L. Lee, and A. P. Mackenzie, Phys. Rev. B **89**, 144504 (2014).
- [51] S. J. Ahn, P. Moon, T.-H. Kim, et al, Science 361,782(2018).
- [52] W. Yao, E. Wang, C. Bao, et al, PNAS 115,6928 (2018).

I. THE REAL-SPACE PERTURBATIVE THEORY

Let's start from the following positive-U Hubbard model on the Penrose lattice,

$$\mathcal{H} = - \sum_{ij\sigma} t_{ij} c_{i\sigma}^\dagger c_{j\sigma} + U \sum_{\mathbf{i}} n_{\mathbf{i}\uparrow} n_{\mathbf{i}\downarrow} - \mu \sum_{i\sigma} n_{i\sigma}. \quad (\text{A1})$$

To treat with this interacting system, let's first investigate the tight-binding (TB) model in its kinetic-energy part, which can be diagonalized as

$$\mathcal{H}_{\text{TB}} = - \sum_{ij\sigma} t_{ij} c_{i\sigma}^\dagger c_{j\sigma} - \mu \sum_{i\sigma} n_{i\sigma} = \sum_m (\epsilon_m - \mu) c_{m\sigma}^\dagger c_{m\sigma} \equiv \sum_m \tilde{\epsilon}_m c_{m\sigma}^\dagger c_{m\sigma} \quad (\text{A2})$$

Here the index m labels the eigen state on the Penrose lattice, and $c_{m\sigma} = \sum_{\mathbf{i}} \xi_{im} c_{i\sigma}$, with ξ_{im} representing for the wave function for the state m . In the following, we shall perform a real-space perturbative treatment on the Hubbard interaction.

The Matsubara single-particle Green's function is defined as,

$$\mathcal{G}_{ij\sigma\sigma'}(\tau_1, \tau_2) = - \langle T_\tau c_{i\sigma}(\tau_1) c_{j\sigma'}^\dagger(\tau_2) \rangle = \mathcal{G}_{ij\sigma\sigma'}(\tau_1 - \tau_2), \quad (\text{A3})$$

with $c_{i\sigma}(\tau) \equiv e^{\mathcal{H}\tau} c_{i\sigma} e^{-\mathcal{H}\tau}$, and $\langle \dots \rangle \equiv \text{Tr}[\rho \dots]$ denotes the thermal average at the temperature T with $\beta = 1/(k_B T)$. This Green's function can be Fourier transformed to the imaginary-frequency space as

$$\mathcal{G}_{ij\sigma\sigma'}(i\omega_n) \equiv \int_0^\beta e^{i\omega_n \tau} \mathcal{G}_{ij\sigma\sigma'}(\tau) d\tau \quad (\text{A4})$$

In the case of $U = 0$, we obtain the bare single-particle Green's function in the eigen basis as

$$\mathcal{G}_{ml\sigma\sigma'}^{(0)}(i\omega_n) = \frac{\delta_{ml} \delta_{\sigma\sigma'}}{i\omega_n - \tilde{\epsilon}_m}, \quad (\text{A5})$$

which is Fourier transformed to the real space as

$$\mathcal{G}_{ij\sigma\sigma'}^{(0)}(i\omega_n) = \sum_m \frac{\xi_{im} \xi_{jm} \delta_{\sigma\sigma'}}{i\omega_n - \tilde{\epsilon}_m}, \quad (\text{A6})$$

where $\omega_n = (2n + 1)\pi/\beta$ is the fermion frequency.

Let's define the real-space susceptibility function

$$\chi_{ij}(\tau) \equiv \langle T_\tau c_{i\sigma}^\dagger(\tau) c_{i\sigma'}(\tau) c_{j\sigma'}^\dagger c_{j\sigma} \rangle_{0,c} = \langle T_\tau c_{i\uparrow}^\dagger(\tau) c_{i\uparrow}(\tau) c_{j\uparrow}^\dagger c_{j\uparrow} \rangle_{0,c}. \quad (\text{A7})$$

Here we only consider the connected Feynman's diagrams in the bare level. Employing Wick's theorem and Eq. (A6), Eq. (A7) can be evaluated, whose Fourier transformation to the imaginary-frequency space is given as

$$\chi_{ij}(i\Omega_n) = \sum_{ml} \xi_{im} \xi_{jm} \xi_{il} \xi_{jl} \frac{n_F(\tilde{\epsilon}_m) - n_F(\tilde{\epsilon}_l)}{i\Omega_n + \tilde{\epsilon}_l - \tilde{\epsilon}_m}, \quad (\text{A8})$$

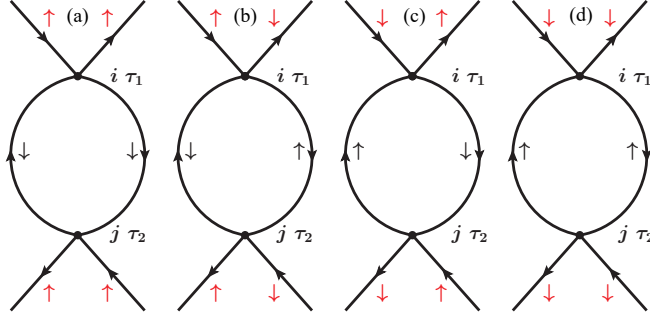


Figure A1. (Color online) Feynman diagrams for the four second-order perturbative processes of exchanging particle-hole fluctuations.

where $\Omega_n = 2n\pi/\beta$ is the boson frequency.

In the Kohn-Luttinger mechanism[1, 2], two electrons at the Fermi level acquire an effective interaction through exchanging the particle-hole fluctuations. There are four relevant second-order processes at the bare-susceptibility level for this mechanism, which are described by the four Feynman's diagrams shown in Fig. A1, leading to the following effective Hamiltonian,

$$\mathcal{H}_{eff} = - \sum_{ij\sigma} t_{ij} c_{i\sigma}^\dagger c_{j\sigma} + U \sum_{\mathbf{i}} n_{i\uparrow} n_{i\downarrow} - \mu \sum_{i\sigma} n_{i\sigma} - (U^2/2) \sum_{ij\sigma\sigma'} \chi_{ij} c_{i\sigma}^\dagger c_{i\sigma'} c_{j\sigma'}^\dagger c_{j\sigma}, \quad (\text{A9})$$

with $\chi_{ij} \equiv \chi_{ij}(i\Omega_n = 0)$. In the following, we shall perform a mean-field (MF) study on Eq.(A9).

As the effective interaction (A9) is invariant under spin-SU(2) transformation, we can perform the MF decoupling in the singlet and triplet channels separately. In the singlet channel Eq. (A9) is MF decoupled as

$$\begin{aligned} \mathcal{H}_{mf}^s &= \sum_{m\sigma} \tilde{\epsilon}_m c_{m\sigma}^\dagger c_{m\sigma} + U \left(\sum_{\mathbf{i}} \Delta_{\mathbf{i}}^{s\dagger} \langle \Delta_{\mathbf{i}}^s \rangle + h.c. - |\langle \Delta_{\mathbf{i}}^s \rangle|^2 \right) + \frac{U^2}{2} (\Delta_{ij}^{s\dagger} \langle \Delta_{ij}^s \rangle + h.c. - |\langle \Delta_{ij}^s \rangle|^2) \chi_{ij} \\ &\equiv \sum_{m,\sigma} \tilde{\epsilon}_m c_{m\sigma}^\dagger c_{m\sigma} + \sum_{m,n} \tilde{\Delta}_{mn}^s c_{m\uparrow}^\dagger c_{n\downarrow}^\dagger + h.c., \end{aligned} \quad (\text{A10})$$

with

$$\Delta_{\mathbf{i}}^{s\dagger} = c_{i\uparrow}^\dagger c_{i\downarrow}^\dagger, \quad (\text{A11})$$

$$\Delta_{ij}^{s\dagger} = \frac{1}{\sqrt{2}} (c_{i\uparrow}^\dagger c_{j\downarrow}^\dagger - c_{i\downarrow}^\dagger c_{j\uparrow}^\dagger), \quad (\text{A12})$$

The MF decoupling of Eq. (A9) in the triplet channel can be performed in three channels with the following three order parameters,

$$\Delta_{ij}^{t\dagger}(1,1) = c_{i\uparrow}^\dagger c_{j\uparrow}^\dagger, \quad (\text{A13})$$

$$\Delta_{ij}^{t\dagger}(1,0) = \frac{1}{\sqrt{2}} (c_{i\uparrow}^\dagger c_{j\downarrow}^\dagger + c_{i\downarrow}^\dagger c_{j\uparrow}^\dagger), \quad (\text{A14})$$

$$\Delta_{ij}^{t\dagger}(1,-1) = c_{i\downarrow}^\dagger c_{j\downarrow}^\dagger, \quad (\text{A15})$$

which represents for the triplet-pairing components with the total S_z of the Cooper pair to be $\hbar, 0$ and $-\hbar$ respectively. Due to the spin-SU(2) symmetry, these three channels are exactly degenerate, which allows that we can only study one component, e.g. the (1,0) component, among the three ones. The MF decoupling in this channel reads as

$$\begin{aligned} \mathcal{H}_{mf}^t &= \sum_{m\sigma} \tilde{\epsilon}_m c_{m\sigma}^\dagger c_{m\sigma} - \frac{U^2}{2} (\Delta_{ij}^{t\dagger} \langle \Delta_{ij}^t \rangle + h.c. - |\langle \Delta_{ij}^t \rangle|^2) \chi_{ij} \\ &\equiv \sum_{m,\sigma} \tilde{\epsilon}_m c_{m\sigma}^\dagger c_{m\sigma} + \sum_{m,n} \tilde{\Delta}_{mn}^t c_{m\uparrow}^\dagger c_{n\downarrow}^\dagger + h.c., \end{aligned} \quad (\text{A16})$$

with $\Delta^{t\dagger}$ to be the abbreviation of the $\Delta^{t\dagger}(1,0)$ in Eq. (A14). To make the calculation feasible, we constrain the summation of energy within a small window, ΔE , around the chemical potential μ .

The BdG Hamiltonians for both the singlet and the triplet (1,0) channels can be written as,

$$\mathcal{H}_{BdG} = \begin{pmatrix} c_{\uparrow}^{\dagger} & c_{\downarrow} \end{pmatrix} \begin{pmatrix} \tilde{\epsilon} & \tilde{\Delta} \\ \tilde{\Delta}^{\dagger} & -\tilde{\epsilon} \end{pmatrix} \begin{pmatrix} c_{\uparrow} \\ c_{\downarrow}^{\dagger} \end{pmatrix} \equiv X^{\dagger} H_{BdG} X, \quad (\text{A17})$$

where c_{σ} is an abbreviation of $(c_{1\sigma}, \dots, c_{L\sigma})$ and L is the number of energy levels in the truncated energy window. The BdG Hamiltonian can be diagonalized as

$$\mathcal{H}_{BdG} = \sum_{m=1}^{2L} E_m \gamma_m^{\dagger} \gamma_m, \quad (\text{A18})$$

with $X = \omega \gamma$, where ω is the matrix of eigenvectors of H_{BdG} . In the following, we derive the linearized gap equation at the critical temperature T_c , solving which we can obtain T_c and the pairing symmetry. We shall demonstrate the procedure of deriving the gap equation for the singlet channel as an example in the following, while for the triplet (1,0) channel, we shall only give the results.

The $\tilde{\Delta}$ in Eq. (A17) can be self-consistently calculated by expanding $c_{i\sigma}$ by $c_{m\sigma}$ and further by γ_m . For the singlet channel at any finite temperature T , it's obtained as

$$\begin{aligned} \tilde{\Delta}_{mn}^s &= U \sum_{\mathbf{i}} \xi_{im} \xi_{in} \sum_{\substack{m',n'=1 \dots L \\ m'',n''=1 \dots 2L}} \omega_{m'+L,m''}^* \omega_{n',m''} \xi_{im'} \xi_{in'} n_F(E_{m''}) \\ &+ \frac{U^2}{2} \sum_{\mathbf{ij}} \chi_{ij} (\xi_{im} \xi_{jn} + \xi_{in} \xi_{jm}) \sum_{\substack{m',n'=1 \dots L \\ m'',n''=1 \dots 2L}} \omega_{m'+L,m''}^* \omega_{n',m''} \xi_{jm'} \xi_{in'} n_F(E_{m''}). \end{aligned} \quad (\text{A19})$$

Here $n_F(\dots)$ represents the Fermi-Dirac distribution function. Noting that E and ω are implicit functions of $\{\tilde{\Delta}_{mn}^s\}$, the Eq. (A19) is actually a self-consistent equation. In practice, it contain too many variables to optimize the solution of the lowest free energy easily. Alternatively, we consider the temperature just below T_c , where the order parameters are infinitely small and we can treat them perturbatively, as done in the following.

The BdG Hamiltonian is made up with two terms,

$$H_{BdG} = \begin{pmatrix} \tilde{\epsilon} & \\ & -\tilde{\epsilon} \end{pmatrix} + \begin{pmatrix} & \tilde{\Delta} \\ \tilde{\Delta}^{\dagger} & \end{pmatrix}. \quad (\text{A20})$$

When the second term goes to infinitesimal just below T_c , we can take it as perturbation, and calculate the E and ω using perturbation theory. Up to the second-order perturbation, we have

$$E_m = \begin{cases} \tilde{\epsilon}_m + \sum_{n \neq m} \frac{|\tilde{\Delta}_{mn}|^2}{\tilde{\epsilon}_m - \tilde{\epsilon}_n} \approx \tilde{\epsilon}_m, m \leq L, \\ -\tilde{\epsilon}_{m-L} + \sum_{n \neq m} \frac{|\tilde{\Delta}_{mn}|^2}{\tilde{\epsilon}_m - \tilde{\epsilon}_n} \approx -\tilde{\epsilon}_{m-L}, m > L, \end{cases} \quad (\text{A21})$$

$$\omega_{m,n} = \delta_{mn}, \quad m, n \leq L, \quad (\text{A22})$$

$$\omega_{m+L,n} = \frac{\tilde{\Delta}_{nm}^*}{\tilde{\epsilon}_n + \tilde{\epsilon}_m}, \quad m, n \leq L, \quad (\text{A23})$$

$$\omega_{m,n+L} = \frac{\tilde{\Delta}_{mn}}{-\tilde{\epsilon}_n - \tilde{\epsilon}_m}, \quad m, n \leq L, \quad (\text{A24})$$

$$\omega_{m+L,n+L} = \delta_{mn}, \quad m, n \leq L. \quad (\text{A25})$$

Keeping to the first order of $\{\tilde{\Delta}_{mn}^s\}$ on both side of Eq. (A19), we obtain the following linearized gap equation for the order parameters $\{\tilde{\Delta}_{mn}^s\}$,

$$\tilde{\Delta}_{mn}^s = F_{mn,m'n'}^{(s)} \tilde{\Delta}_{m'n'}^s, \quad (\text{A26})$$

where $F_{mn,m'n'}^{(s)}$ is

$$F_{mn,m'n'}^{(s)} = \frac{[n_F(\tilde{\epsilon}_{m'}) - n_F(-\tilde{\epsilon}_n)]}{\tilde{\epsilon}_{m'} + \tilde{\epsilon}_n} \left[U \sum_{\mathbf{i}} \xi_{in} \xi_{im} \xi_{in'} \xi_{im'} + \frac{U^2}{4} \sum_{\mathbf{ij}} \chi_{ij} (\xi_{im} \xi_{jn} + \xi_{in} \xi_{jm}) (m, n \Rightarrow m'n') \right]. \quad (\text{A27})$$

The problem defined in Eq. (A27) now becomes to seek the eigenvector(s) of the matrix $F^{(s)}$ (here we have taken the mn as the row index and the $m'n'$ as the column index) with unit eigenvalue. It is noticed that the $F^{(s)}$ is not Hermitian, so we turn to solve another equivalent eigenvalue problem for an Hermitian matrix. Let's define

$$\tilde{\Delta}_{mn}^{(s/t)} \equiv \tilde{\Delta}_{mn}^{(s/t)} \sqrt{\frac{[n_F(-\tilde{\epsilon}_n) - n_F(\tilde{\epsilon}_m)]}{\tilde{\epsilon}_m + \tilde{\epsilon}_n}}, \quad (\text{A28})$$

then the Eq. (A26) becomes

$$\tilde{\Delta}_{mn}^s = \tilde{F}_{mn,m'n'}^{(s)} \tilde{\Delta}_{m'n'}^s, \quad (\text{A29})$$

with $\tilde{F}^{(s)}$ given by

$$\begin{aligned} \tilde{F}_{mn,m'n'}^{(s)} = & -\sqrt{\frac{[n_F(-\tilde{\epsilon}_n) - n_F(\tilde{\epsilon}_m)]}{\tilde{\epsilon}_m + \tilde{\epsilon}_n}} \left[U \sum_{\mathbf{i}} \xi_{in} \tilde{\xi}_{im} \xi_{in'} \xi_{im'} \right. \\ & \left. + \frac{U^2}{4} \sum_{\mathbf{ij}} \chi_{ij} (\xi_{im} \xi_{jn} + \xi_{in} \xi_{jm}) (m, n \Rightarrow m'n') \right] \sqrt{\frac{[n_F(-\tilde{\epsilon}_{n'}) - n_F(\tilde{\epsilon}_{m'})]}{\tilde{\epsilon}_{m'} + \tilde{\epsilon}_{n'}}}. \end{aligned} \quad (\text{A30})$$

Clearly, the matrix $\tilde{F}^{(s)}$ now becomes real and symmetric, which is therefore Hermitian. Eq. (A27) is the linearized gap equation at T_c for the singlet pairings.

Following the same procedure, we obtain the following linearized gap equation for the triplet pairing,

$$\tilde{\Delta}_{mn}^t = \tilde{F}_{mn,m'n'}^{(t)} \tilde{\Delta}_{m'n'}^t, \quad (\text{A31})$$

$$\tilde{F}_{mn,m'n'}^{(t)} = \sqrt{\frac{[n_F(-\tilde{\epsilon}_n) - n_F(\tilde{\epsilon}_m)]}{\tilde{\epsilon}_m + \tilde{\epsilon}_n}} \left[\frac{U^2}{4} \sum_{\mathbf{ij}} \chi_{ij} (\xi_{im} \xi_{jn} - \xi_{in} \xi_{jm}) (m, n \Rightarrow m'n') \right] \sqrt{\frac{[n_F(-\tilde{\epsilon}_{n'}) - n_F(\tilde{\epsilon}_{m'})]}{\tilde{\epsilon}_{m'} + \tilde{\epsilon}_{n'}}}. \quad (\text{A32})$$

The linearized gap equation Eq.(A26) for the singlet pairings or Eq.(A31) for the triplet pairings takes the form of an eigenvalue problem for the matrix $\tilde{F}^{(s)}$ or $\tilde{F}^{(t)}$. The superconducting critical temperature T_c is the temperature at which the largest eigenvalue of $\tilde{F}^{(s)}$ or $\tilde{F}^{(t)}$ attains 1. The pairing symmetry is determined by the relative gap function $\tilde{\Delta}_{mn}^s$ or $\tilde{\Delta}_{mn}^t$, which is related to the eigenvector $\tilde{\Delta}_{mn}^s$ or $\tilde{\Delta}_{mn}^t$ corresponding to the largest eigenvalue, i.e. 1, of the matrix $\tilde{F}^{(s)}$ or $\tilde{F}^{(t)}$ through the relation (A28). Note that $\tilde{\Delta}_{mn}^s$ or $\tilde{\Delta}_{mn}^t$ only serves as a renormalized gap form factor, and the global pairing amplitude will be enhanced with the decreasing of T below T_c , determined by the minimization of free energy.

II. BASIS FOR CLASSIFICATION OF PAIRING SYMMETRIES

Here, we prove that if the binary gap function $\Delta_{\mathbf{i},\mathbf{j}}$ is the real-space correspondence to a solution of the linearized gap equation Eq. (A26) or Eq. (A31), then $\Delta_{\hat{g}\mathbf{i},\hat{g}\mathbf{j}}$ will also be a real-space gap function corresponding to the solution of the equation with the same critical temperature. As a result, all the gap functions $\{\Delta_{\mathbf{i},\mathbf{j}}^{(\alpha)}\}$ ($\alpha = 1, 2, \dots$) corresponding to the solution of the linearized gap equation with the same critical temperature just form an irreducible representation (IR) of the D_5 point group of the system. This builds the basis for the classification of the pairing symmetries.

Considering each element $g \in D_5$, we have $\hat{P}_g |\mathbf{i}, \sigma\rangle \equiv |\hat{g}\mathbf{i}, \sigma\rangle$, from which we obtain

$$\hat{P}_g c_{\mathbf{i}\sigma} \hat{P}_g^{-1} = c_{\hat{g}\mathbf{i},\sigma}. \quad (\text{A33})$$

Then, the effect of \hat{P}_g acting on an eigenvector of the TB Hamiltonian is given by

$$\hat{P}_g \xi_{\mathbf{i},m} = \xi_{\hat{g}^{-1}\mathbf{i},m}. \quad (\text{A34})$$

On the other hand, as the TB Hamiltonian is invariant under D_5 , its eigenvector(s) corresponding to the same eigenvalue must furnish an IR of the point group. As a result, we have

$$\hat{P}_g \xi_{i,m} = \xi_{\hat{g}^{-1}i,m} \equiv \xi_{\hat{g}^{-1}i,\tilde{m}\tilde{\alpha}} = \sum_{\tilde{\alpha}'} D_{\tilde{\alpha},\tilde{\alpha}'}^{(g,\tilde{m})} \xi_{i,\tilde{m}\tilde{\alpha}'}. \quad (\text{A35})$$

Here we explicitly express the index m of an eigen state with a pair of indices, i.e. $m \equiv \tilde{m}\tilde{\alpha}$, with the first index labeling the energy level and the second one labeling the degenerate eigen state(s) with the same eigen energy. The $D^{(g,\tilde{m})}$ is the matrix corresponding to the element g for the IR furnished by the eigenvector(s) belonging to $\tilde{\epsilon}_{\tilde{m}}$. Making use of the obviously equality, $\chi_{i,j} = \chi_{\hat{g}i,\hat{g}j}$, it is convenient to show that the $F^{(s)}$ is invariant under the following symmetry-group operation,

$$\begin{aligned} \sum_{\tilde{\mu}\tilde{\nu}\tilde{\mu}'\tilde{\nu}'} D_{\tilde{\alpha},\tilde{\mu}}^{(g,\tilde{m})} D_{\tilde{\beta},\tilde{\nu}}^{(g,\tilde{n})} D_{\tilde{\alpha}',\tilde{\mu}'}^{(g,\tilde{m}')} D_{\tilde{\beta}',\tilde{\nu}'}^{(g,\tilde{n}')} F_{\tilde{m}\tilde{\mu}\tilde{n}\tilde{\nu},\tilde{m}'\tilde{\mu}'\tilde{n}'\tilde{\nu}'}^{(s)} &= \frac{[n_F(\tilde{\epsilon}_{\tilde{m}'}) - n_F(-\tilde{\epsilon}_{\tilde{n}'})]}{\tilde{\epsilon}_{\tilde{m}'} + \tilde{\epsilon}_{\tilde{n}'}} \left[U \sum_{\mathbf{i}} \xi_{\hat{g}^{-1}i,\tilde{n}\tilde{\beta}} \xi_{\hat{g}^{-1}i,\tilde{m}\tilde{\alpha}} \xi_{\hat{g}^{-1}i,\tilde{n}'\tilde{\beta}'} \xi_{\hat{g}^{-1}i,\tilde{m}'\tilde{\alpha}'} \right. \\ &\quad \left. + \frac{U^2}{4} \sum_{\mathbf{ij}} \chi_{\hat{g}^{-1}i,\hat{g}^{-1}j} (\xi_{\hat{g}^{-1}i,\tilde{m}\tilde{\alpha}} \xi_{\hat{g}^{-1}j,\tilde{n}\tilde{\beta}} + \xi_{\hat{g}^{-1}i,\tilde{n}\tilde{\beta}} \xi_{\hat{g}^{-1}j,\tilde{m}\tilde{\alpha}}) \times (\tilde{m}\tilde{\alpha}, \tilde{n}\tilde{\beta} \Rightarrow \tilde{m}'\tilde{\alpha}', \tilde{n}'\tilde{\beta}') \right] \\ &= \frac{[n_F(\tilde{\epsilon}_{\tilde{m}'}) - n_F(-\tilde{\epsilon}_{\tilde{n}'})]}{\tilde{\epsilon}_{\tilde{m}'} + \tilde{\epsilon}_{\tilde{n}'}} \left[U \sum_{\mathbf{i}} \xi_{i,\tilde{n}\tilde{\beta}} \xi_{i,\tilde{m}\tilde{\alpha}} \xi_{i,\tilde{n}'\tilde{\beta}'} \xi_{i,\tilde{m}'\tilde{\alpha}'} + \frac{U^2}{4} \sum_{\mathbf{ij}} \chi_{\mathbf{ij}} (\xi_{i,\tilde{m}\tilde{\alpha}} \xi_{j,\tilde{n}\tilde{\beta}} + \xi_{i,\tilde{n}\tilde{\beta}} \xi_{j,\tilde{m}\tilde{\alpha}}) (\tilde{m}\tilde{\alpha}, \tilde{n}\tilde{\beta} \Rightarrow \tilde{m}'\tilde{\alpha}', \tilde{n}'\tilde{\beta}') \right] \\ &= F_{\tilde{m}\tilde{\alpha}\tilde{n}\tilde{\beta},\tilde{m}'\tilde{\alpha}'\tilde{n}'\tilde{\beta}'}^{(s)}, \end{aligned} \quad (\text{A36})$$

and so as $F^{(t)}$. From Eq. (A36), it can be easily proved that if $\tilde{\Delta}_{mn}^{s/t} \equiv \tilde{\Delta}_{\tilde{m}\tilde{\alpha}\tilde{n}\tilde{\beta}}^{s/t}$ is a solution of Eq. (A26) or Eq. (A31), then $(\hat{P}_g \tilde{\Delta}_{\tilde{m}\tilde{\alpha}\tilde{n}\tilde{\beta}}^{s/t}) \equiv \sum_{\tilde{\mu}\tilde{\nu}} D_{\tilde{\alpha},\tilde{\mu}}^{(g,\tilde{m})} D_{\tilde{\beta},\tilde{\nu}}^{(g,\tilde{n})} \tilde{\Delta}_{\tilde{m}\tilde{\mu}\tilde{n}\tilde{\nu}}^{s/t}$ would also be a solution of Eq. (A26) or Eq. (A31) corresponding to the same T_c . Let $\Delta_{\mathbf{ij}}^{s/t}$ be the real-space correspondence of $\tilde{\Delta}_{mn}^{s/t}$ via the relation $\Delta_{\mathbf{ij}}^{s/t} = \sum_{mn} \tilde{\Delta}_{mn}^{s/t} \xi_{im} \xi_{jn}$, then from Eq. (A35) it's easily obtained that the real-space correspondence of $\hat{P}_g \tilde{\Delta}_{mn}^{s/t}$ is $\Delta_{\hat{g}i,\hat{g}j}^{s/t}$. Therefore, if $\Delta_{\mathbf{ij}}$ is a real-space solution of the linearized gap equation with a T_c , then $\Delta_{\hat{g}i,\hat{g}j}$ would also be a solution with the same T_c . As a result, all the real-space solutions $\{\Delta_{\mathbf{ij}}^{(\alpha)}\}$ corresponding to the same T_c furnish an IR of the point group, expressed as,

$$\Delta_{\hat{g}i,\hat{g}j}^{(\alpha)} = \sum_{\alpha'} D_{\alpha,\alpha'}^{(g)} \Delta_{i,j}^{(\alpha')}. \quad (\text{A37})$$

Here $D^{(g)}$ is the representation matrix corresponding to the element $g \in D_5$. From the IR that $\{D^{(g)}\}$ belongs to, we can classify the pairing symmetry of the group of pairing states with gap functions $\{\Delta_{\mathbf{ij}}^{(\alpha)}\}$.

III. TOPOLOGICAL INVARIANT

Based on the K -theory, the Chern number for a finite-size system can be expressed as the following pseudo-spectrum invariant index[3, 4],

$$C_{ps} = \frac{1}{2} \text{Sig} \begin{pmatrix} X & Y + iH \\ Y - iH & -X \end{pmatrix}, \quad (\text{A38})$$

where Sig represents the difference between the numbers of positive and negative eigenvalues of the matrix acted on, X and Y are position-operator matrices with X defined by $X = \text{diag}(x_1, x_1, x_1, x_1, \dots, x_N, x_N, x_N, x_N)$ and Y defined similarly. The BdG-Hamiltonian matrix H is defined as

$$H = \begin{pmatrix} h_{11} & h_{12} & \cdots & h_{1N} \\ h_{21} & h_{22} & \cdots & h_{2N} \\ \vdots & \vdots & \ddots & \vdots \\ h_{N1} & h_{N2} & \cdots & h_{NN} \end{pmatrix}, \quad (\text{A39})$$

in which h is the matrix of local BdG-Hamiltonian defined as

$$\mathcal{H}_{\text{BdG}} = \sum_{ij} (c_{i\uparrow}^\dagger c_{i\downarrow}^\dagger c_{i\uparrow} c_{i\downarrow}) h_{ij} (c_{j\uparrow}^\dagger c_{j\downarrow}^\dagger c_{j\uparrow} c_{j\downarrow})^\dagger. \quad (\text{A40})$$

From the above introduced definition of C_{ps} , it's shown below that C_{ps} has two universal properties.

Firstly, any global unitary transformation will not change C_{ps} . Such unitary transformation is embodied as a site-independent unitary matrix u performed on all the h_{ij} , leading to $h_{ij} \rightarrow \tilde{h}_{ij} \equiv u h_{ij} u^\dagger$. Defining the unitary matrix $U = \text{diag}(u, u, \dots, u)$, it can be easily verified that

$$U \begin{pmatrix} X & Y + iH \\ Y - iH & -X \end{pmatrix} U^\dagger = \begin{pmatrix} X & Y + i\tilde{H} \\ Y - i\tilde{H} & -X \end{pmatrix}, \quad (\text{A41})$$

which suggests that the global unitary transformation will not change C_{ps} .

From the above property, it's easily known that the two TRS-breaking triplet pairing states have the same Chern number: one is described by the pairing term $\sum_{ij} \Delta_{ij} (c_{i\uparrow} c_{j\downarrow} + c_{i\downarrow} c_{j\uparrow}) + h.c.$, i.e. the $(1, 0)$ component; the other is described by $\sum_{ij} \Delta_{ij} (c_{i\uparrow} c_{j\uparrow} \pm c_{i\downarrow} c_{j\downarrow}) + h.c.$, i.e. the $(1, 1) \pm (1, -1)$ component. Obviously, the two chiral pairing states are mutually related by a global spin-SU(2) rotation (i.e. $\hat{s}_z \rightarrow \hat{s}_x$, for the case of $(1, 1) - (1, -1)$) followed by a spin-dependent U(1)-gauge rotation (i.e. $c_\downarrow \rightarrow i c_\downarrow$, for the case of $(1, 1) + (1, -1)$), which makes them share the same Chern number. Further more, the matrix in the right side of Eq.(A38) for the $(1, 1) \pm (1, -1)$ state is block-diagonalized into the spin-up block and the spin-down one, suggesting that the Chern number of the two chiral triplet pairing state is twice as much as the one for a spinless system with the same pairing form factor.

Secondly, the C_{ps} for a pairing state and that for its time-reversal (TR) conjugate is different by a sign. This property is proved as follow. Under TR transformation, we have

$$\begin{aligned} T h_{ij} T^{-1} &= \begin{pmatrix} -i\sigma_y & 0 \\ 0 & -i\sigma_y \end{pmatrix} h_{ij}^* \begin{pmatrix} i\sigma_y & 0 \\ 0 & i\sigma_y \end{pmatrix} = \begin{pmatrix} \sigma_y & 0 \\ 0 & \sigma_y \end{pmatrix} h_{ij}^* \begin{pmatrix} \sigma_y & 0 \\ 0 & \sigma_y \end{pmatrix} \\ &= - \begin{pmatrix} \sigma_y & 0 \\ 0 & \sigma_y \end{pmatrix} \begin{pmatrix} 0 & I_2 \\ I_2 & 0 \end{pmatrix} h_{ij} \begin{pmatrix} 0 & I_2 \\ I_2 & 0 \end{pmatrix} \begin{pmatrix} \sigma_y & 0 \\ 0 & \sigma_y \end{pmatrix} = - \begin{pmatrix} 0 & \sigma_y \\ \sigma_y & 0 \end{pmatrix} h_{ij} \begin{pmatrix} 0 & \sigma_y \\ \sigma_y & 0 \end{pmatrix}. \end{aligned} \quad (\text{A42})$$

Here we have used the particle-hole symmetry of the BdG-Hamiltonian (in the third “=” above). Since $\begin{pmatrix} 0 & \sigma_y \\ \sigma_y & 0 \end{pmatrix}$ is a site-independent unitary transformation, the $C_{ps}(H)$ is changed to $C_{ps}(-H)$ after the TR transformation. According to the following derivation,

$$\begin{aligned} \text{Sig} \begin{pmatrix} X & Y - iH \\ Y + iH & -X \end{pmatrix} &= -\text{Sig} \begin{pmatrix} -X & -Y + iH \\ -Y - iH & X \end{pmatrix} = -\text{Sig} \begin{pmatrix} 0 & I_{4N} \\ I_{4N} & 0 \end{pmatrix} \begin{pmatrix} -X & -Y + iH \\ -Y - iH & X \end{pmatrix} \begin{pmatrix} 0 & I_{4N} \\ I_{4N} & 0 \end{pmatrix} \\ &= -\text{Sig} \begin{pmatrix} X & -Y - iH \\ -Y + iH & -X \end{pmatrix} \\ &= -\text{Sig} \begin{pmatrix} I_{4N} & 0 \\ 0 & -I_{4N} \end{pmatrix} \begin{pmatrix} X & -Y - iH \\ -Y + iH & -X \end{pmatrix} \begin{pmatrix} I_{4N} & 0 \\ 0 & -I_{4N} \end{pmatrix} = -C_{ps}(H), \end{aligned} \quad (\text{A43})$$

we know that $C_{ps}(H) = -C_{ps}(THT^{-1})$.

From the above property, we can know that the Chern numbers of all TRI pairing states are zero, because they should be equal to their opposite numbers. Therefore, all 1D-IR pairing states have zero Chern numbers, as the gap functions in these pairing states are real, which are TRI. Further more, the TRI helical triplet pairing state with pairing term $\sum_{ij} (\Delta_{ij} c_{i\uparrow} c_{j\uparrow} + \Delta_{ij}^* c_{i\downarrow} c_{j\downarrow}) + h.c.$ and its gauge-rotated state $\sum_{ij} (\Delta_{ij} c_{i\uparrow} c_{j\uparrow} - \Delta_{ij}^* c_{i\downarrow} c_{j\downarrow}) + h.c.$ (with $c_\downarrow \rightarrow i c_\downarrow$) should also have zero Chern numbers.

Besides the above two universal properties, there is another important question to ask: for a triplet and a singlet pairing states with the same gap form factor except for the different exchanging parities, what's the relation between their Chern numbers? Obviously, the two states share the same pairing symmetry, but possess different total spins for the Cooper pair. Our numerical calculations on a lattice with 3466 sites and with restricted hopping integrals up to the third nearest neighbor show that such two pairing states share the same Chern numbers, although their total spins of Cooper pair are different, suggesting that the Chern number is only related to the pairing symmetry.

IV. THE CURRENT OPERATOR

The α - component ($\alpha = x, y$) of the vectorial current operator $\hat{\mathbf{J}}_{\mathbf{i}}$ at a specific site \mathbf{i} is defined as

$$\hat{J}_{i\alpha}[\mathbf{A}] = -\frac{\delta\hat{\mathcal{H}}[\mathbf{A}]}{\delta A_{i\alpha}} = -\frac{\delta\hat{\mathcal{H}}_{\text{TB}}[\mathbf{A}]}{\delta A_{i\alpha}}, \quad (\text{A44})$$

where \mathbf{A} is the vector potential, which appears in $\hat{\mathcal{H}}[\mathbf{A}]$ through a modification of the $\hat{\mathcal{H}}_{\text{TB}}$ into

$$\hat{\mathcal{H}}_{\text{TB}}[\mathbf{A}] = -\sum_{\mathbf{ij}\sigma} t_{\mathbf{ij}} \exp(i \int_{\mathbf{i}}^{\mathbf{j}} \mathbf{A} \cdot d\mathbf{l}) c_{i\sigma}^\dagger c_{j\sigma}. \quad (\text{A45})$$

In our linear-response consideration of the superfluid density, the field \mathbf{A} is a weak and smooth field. In such a limit, we can approximate Eq. (A45) as

$$\hat{\mathcal{H}}_{\text{TB}}[\mathbf{A}] \approx -\sum_{\mathbf{ij}\sigma} t_{\mathbf{ij}} [1 + i(\mathbf{A}_{\mathbf{i}} + \mathbf{A}_{\mathbf{j}}) \cdot \mathbf{R}_{\mathbf{ij}}/2 - [(\mathbf{A}_{\mathbf{i}} + \mathbf{A}_{\mathbf{j}}) \cdot \mathbf{R}_{\mathbf{ij}}]^2/8] c_{i\sigma}^\dagger c_{j\sigma}. \quad (\text{A46})$$

Substituting Eq. (A46) to Eq. (A44), we obtain the formula of the α - component of the current operator,

$$\hat{J}_{i\alpha}[\mathbf{A}] = \frac{i}{2} \sum_{\mathbf{l}\sigma} t_{\mathbf{il}} R_{\mathbf{il},\alpha} c_{i\sigma}^\dagger c_{\mathbf{l}\sigma} + h.c. - \frac{1}{2} \sum_{\mathbf{l}\sigma} t_{\mathbf{il}} R_{\mathbf{il},\alpha} (\mathbf{R}_{\mathbf{il}} \cdot \mathbf{A}_{\mathbf{i}}) c_{i\sigma}^\dagger c_{\mathbf{l}\sigma} + h.c., \quad (\text{A47})$$

where $R_{\mathbf{il},\alpha}$ is the α - component of the relative position $\mathbf{R}_{\mathbf{il}} \equiv \mathbf{r}_{\mathbf{l}} - \mathbf{r}_{\mathbf{i}}$. The current operator consists of two parts, one is the constant part called as the paramagnetic current and the other is the part proportional to the vector potential called as the diamagnetic current.

Note that the current operator expressed as Eq.(A47) is TR odd,

$$T\hat{\mathbf{J}}_{\mathbf{i}}T^{-1} = -\hat{\mathbf{J}}_{\mathbf{i}}.$$

Therefore, the expectation value $\langle \hat{\mathbf{J}}_{\mathbf{i}} \rangle$ in a TRI pairing state with $\mathbf{A} = 0$ should always be zero. However, in a TRS-breaking chiral pairing state, it's possible to have $\langle \hat{\mathbf{J}}_{\mathbf{i}}[\mathbf{A} = 0] \rangle \neq 0$, suggesting the possibility of the spontaneous symmetry broken. But the total super current $\langle \sum_{\mathbf{i}} \hat{\mathbf{J}}_{\mathbf{i}}[\mathbf{A} = 0] \rangle$ should be zero with $\mathbf{A} = 0$, otherwise the macro superfluid density should be infinity.

Then, let's study the superfluid density, which is a tensor defined as

$$\rho_s^{\alpha\beta} \equiv \lim_{A_\beta \rightarrow 0} \frac{-\langle A_\beta | \hat{J}_\alpha | A_\beta \rangle}{A_\beta}. \quad (\text{A48})$$

Here \hat{J}_α is the α -component of the total super current per site defined as $\hat{\mathbf{J}} = \frac{1}{N} \sum_{\mathbf{i}} \hat{\mathbf{J}}_{\mathbf{i}}$. In the following, we shall prove that this tensor is diagonal and isotropic, i.e. $\rho_s^{\alpha\beta} = \rho_0 \delta_{\alpha\beta}$, for all the pairing symmetries listed in the Table. I of the main text.

Let's consider an infinitesimal \mathbf{A} imposed on the system, which will induce a super current $\mathbf{J} \equiv \langle \hat{\mathbf{J}} \rangle$, whose two components satisfy,

$$\begin{pmatrix} J_x \\ J_y \end{pmatrix} = - \begin{pmatrix} \rho_{xx} & \rho_{xy} \\ \rho_{yx} & \rho_{yy} \end{pmatrix} \begin{pmatrix} A_x \\ A_y \end{pmatrix}. \quad (\text{A49})$$

Let's consider an arbitrary symmetry operation $g \in D_5$ acted on the system. For any pairing symmetry listed in the Table. I of the main text, the transformed gap function by g can be expressed as $\hat{P}_g \Delta_{mn} \hat{P}_g^{-1} = e^{i\theta_g} \Delta_{mn}$, where θ_g is the angle according to the specific representation. Therefore, the transformed Hamiltonian $\hat{P}_g \hat{\mathcal{H}}_{\text{BCS}} \hat{P}_g^{-1}$ can be recovered to the original one by a succeeding global gauge transformation, $c_{i,\sigma} \rightarrow e^{-i\theta_g/2} c_{i,\sigma}$, which will not change the superfluid density. As a result, after the $g \in D_5$ symmetry operation acted on the system, the superfluid density tensor $\begin{pmatrix} \rho_{xx} & \rho_{xy} \\ \rho_{yx} & \rho_{yy} \end{pmatrix}$ doesn't alert. On the other hand, the vectorial current and vector potential are transformed as

$$\begin{pmatrix} J_x \\ J_y \end{pmatrix} \rightarrow R_g \begin{pmatrix} J_x \\ J_y \end{pmatrix}, \quad \begin{pmatrix} A_x \\ A_y \end{pmatrix} \rightarrow R_g \begin{pmatrix} A_x \\ A_y \end{pmatrix}. \quad (\text{A50})$$

As a result, we have $[\rho_s, R_g] = 0$ for any $g \in D_5$. There are two types of R_g ,

$$R_{\hat{C}_{\frac{2\pi n}{5}}} = \begin{pmatrix} \cos \theta_n & -\sin \theta_n \\ \sin \theta_n & \cos \theta_n \end{pmatrix} = \cos \theta_n I - i \sin \theta_n \sigma_y, R_{\hat{\sigma}_x} = \begin{pmatrix} 1 & 0 \\ 0 & -1 \end{pmatrix} = \sigma_z. \quad (\text{A51})$$

Setting $\rho_s = \alpha I + \beta \sigma_x + \mu \sigma_y + \nu \sigma_z$, it can be verified that $[\rho_s, R_g] = 0 \rightarrow \beta = \mu = \nu = 0$. As a result, we have $\rho_s^{\alpha\beta} = \rho_0 \delta_{\alpha\beta}$. Our numerical calculation agrees with this theoretical result, and the linear response along the direction x is shown in Fig. A2, which suggests a nonzero superfluid density.

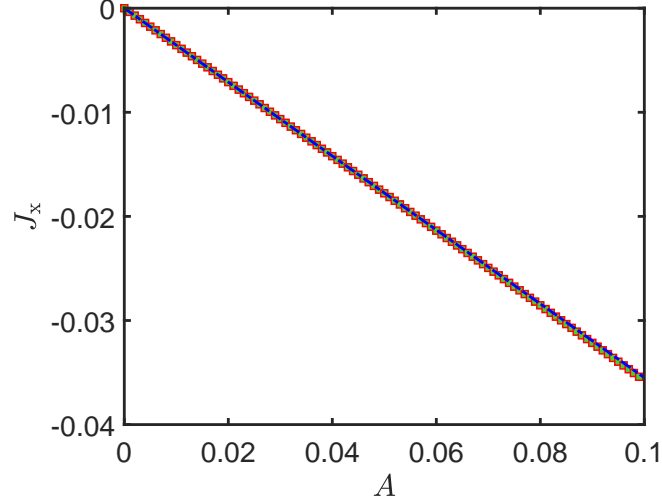


Figure A2. (Color online) Linear response of the macro super current to an imposed vector potential \mathbf{A} along the x - direction in a single $p + ip/g + ig$ state at the doping 0.955 and $U/W_D \approx 0.129$.

-
- [1] W. Kohn and J. M. Luttinger, Phys. Rev. Lett. **15**, 524 (1965).
 - [2] M. A. Baranov, A. V. Chubukov, and M. Yu. Kagan, Int. J. Mod. Phys. B **06**, 2471 (1992).
 - [3] T. A. Loring, Ann. Phys. (N. Y). **356**, 383 (2015).
 - [4] I. C. Fulga, D. I. Pikulin, and T. A. Loring, Phys. Rev. Lett. **116**, 257002 (2016).
-